absence of buoyancy forces, is stable to small disturbances, in contradiction to the experimental results of Block. The cellular instability which he observed perhaps was the result of some small but unknown surface contamination or, possibly, it can only be explained by nonlinear stability theory. It also might be useful to repeat the experiments to determine the range of parameters over which the observed instability occurs.

References

[1] Block, M.J., "Surface Tension as the Cause of Benard Cells and Surface Deformation in a Liquid Film," *Nature,* Vol. 178, Sept. 22, 1956, pp. 650, 651.

[2] Pearson, J.R.A., "On Convection Cells Induced by Surface Tension," *Journal of Fluid Mechanics*, Vol. 4, Sept. 1958, pp. 489-500.

[3] Scriven, L.E. and Sternling, C.V., "On Cellular Convection Driven by Surface Tension Gradients: Effects of Mean Surface Tension and Surface Viscosity," *Journal of Fluid Mechanics,* Vol. 19, July 1964, pp. 321-340.

[4] Chandrasekhar, S., *Hydrodynamic and Hydromagnetic Stability,* Oxford, London, 1961.

[5] Vidal, A. and Acrivos, A., "Nature of the Neutral State in Surface-Tension Driven Convection," *Physics of Fluids*, Vol. 9, March 1966, pp. 615, 616.

[6] Takashima, M., "Nature of the Neutral State in Convective Instability Induced by Surface Tension and Buoyancy," *Journal of the Physical Society of Japan*, Vol. 28, March 1970, p. 810.

AIAA 81-1476R

Simultaneous Solution of the Inviscid Flow and Boundary Layers for Compressor Cascades

H. L. Moses* and S. B. Thomason†
Virginia Polytechnic Institute and State University, Blacksburg, Virginia
and
R. R. Jones III‡
Sverdrup Technology, Inc., Tullahoma, Tennessee

Nomenclature

A,B,C,D	= coefficients in linear equations
H	= boundary-layer shape factor δ^*/θ
r	= radius
s	= distance along airfoil surface
U	= boundary-layer edge velocity
x	= longitudinal coordinate
y	= transverse coordinate
δ^*	= boundary-layer displacement thickness
ψ	= stream function
θ	= boundary-layer momentum thickness

Subscripts

dn	= downstream
i,j	= grid locations
p	= pressure side
s	= suction side
te	= trailing edge
up	= upstream

Presented as Paper 81-1476 at the AIAA/SAE/ASME 17th Joint Propulsion Conference, Colorado Springs, Colo., July 27-29, 1981; submitted Aug. 12, 1981; revision received March 2, 1982.

*Professor, Mechanical Engineering Department.
†Assistant Professor. Member AIAA.
‡Research Engineer, AEDC Group. Member AIAA.

Introduction

THE solution of inviscid flow through axial-flow compressor cascades is well developed and often used in some aspects of design. Prediction of the total pressure loss and stall, however, requires consideration of the turbulent boundary layer. The combined solution of the inviscid flow and the boundary layers is generally difficult, especially where there is a strong interaction between the two, and is not often used.

When separation is involved, a straightforward iteration between the boundary layer and inviscid flow fails because of the singular behavior of the equations (see Ref. 1, for example). The general problem of separation has received a great deal of attention recently, and a number of approaches, including simultaneous methods, inverse boundary-layer calculations, and fully elliptic procedures, have been published.

The purpose of the present Note is to describe an approximate procedure for calculating the boundary layers in compressor cascades simultaneously with the inviscid flow. To best describe the basic approach, it is presented here in its simplest form, with a stream function equation for the inviscid flow and an integral method for the boundary layers.

The procedure has been applied to diffuser flow with laminar and turbulent boundary layers[1,2] and to a compressor rotor.[3]

Analysis

In the present analysis, it is assumed that the flow can be divided into an inviscid region and relatively thin viscous layers. To be consistent with boundary-layer theory, it is assumed that the pressure is determined by the inviscid flow. The patching between the two layers is accomplished by a simultaneous solution using successive line relaxation. The solution is matched at the displacement thickness of the boundary layer.

A finite-difference method is used for the inviscid flow region with the simple rectangular grid system shown in Fig. 1. It is advantageous for the boundary-layer calculation to align one coordinate as nearly as possible with the flow direction. For line relaxation, the stream function equation is written for the unknown values at a given longitudinal position, assuming that upstream values are known from the previous step and downstream values from the previous iteration. These equations can be written

$$A_j\psi_{i,j-1}+B_j\psi_{i,j}+C_j\psi_{i,j+1}=D_j \tag{1}$$

The boundary layers on the airfoil surfaces are treated with a simple integral technique. Almost all integral methods, for laminar and turbulent flow, can be arranged to give two equations of the form

$$B_1\mathrm{d}H+C_1\mathrm{d}\delta^*=D_{11} \tag{2}$$

and

$$A_2\mathrm{d}H+B_2\mathrm{d}\delta^*+C_2\mathrm{d}U=D_{22} \tag{3}$$

In finite-difference form, with upstream differencing, Eqs. (2) and (3) can be written

$$B_1H_i+C_1\delta_i^*=D_1 \tag{4}$$

and

$$A_2H_i+B_2\delta_i^*+C_2U_i=D_2 \tag{5}$$

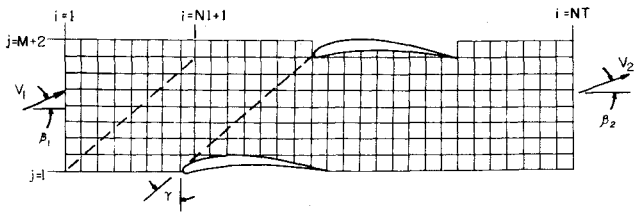

Fig. 1 Grid system for finite-difference calculations.

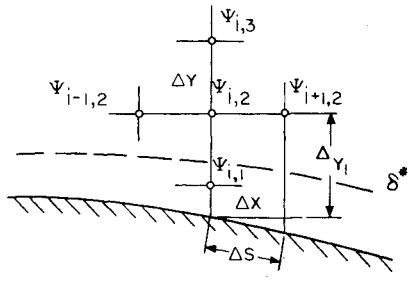

Fig. 2 Grid system at boundary layer.

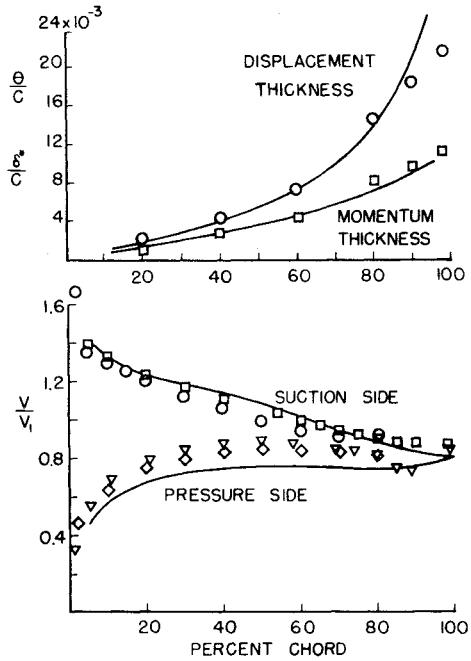

Fig. 3 Comparison of calculations with experimental data for NACA 65-410 airfoil and data from Refs. 4 and 5; spacing/chord = 1.25, $\beta_1 = 17$ deg.

In the work presented here, a very simple method was used for purposes of illustration. The method is based on the momentum and kinetic energy integral equations.

For the first grid point outside the boundary layer (Fig. 2), the stream function for the point inside of the boundary layer is eliminated from Eq. (1) by the first-order approximation for the velocity

$$\psi_{i,1} = \psi_{i,2} - \Delta y U_i \Big/ \left(\frac{ds}{dx}\right)_i \tag{6}$$

The edge velocity is related to the displacement thickness by the first-order approximation

$$U_i = (\psi_{i,2} - \psi_{\delta^*}) \Big/ \left[\left(\Delta y_1 \frac{dx}{ds}\right)_i - \delta_i^*\right] \tag{7}$$

Equation (7) is differentiated with upstream differencing to obtain a linear relation

$$A_3 \delta_i^* + B_3 U_i + C_3 \psi_{i,2} = D_3 \tag{8}$$

where

$$A_3 = U_{i-1}$$

$$B_3 = -\left[\left(\Delta y_1 \frac{dx}{ds}\right)_{i-1} - \delta_{i-1}^*\right]$$

$$C_3 = 1.0$$

$$D_3 = \psi_{i-1,2} - U_{i-1}\left[2\left(\Delta y_1 \frac{dx}{ds}\right)_{i-1} - 2\delta_{i-1}^* - \left(\Delta y_1 \frac{dx}{ds}\right)_i\right] \tag{9}$$

Along the displaced boundaries of the airfoils, the stream function is assumed constant. For convenience the difference is chosen to result in an upstream velocity of 1.0. On the upstream boundary, $i=1$, and on the top boundary, $j=M+2$ for $i=1$ to $N1$, the stream function is assumed linear and is determined from the specified inlet angle and the value at $i=1, j=1$. Except for the linear regions and the blade surface, a repetitive condition is used for the top and bottom boundaries. In this case

$$\psi_{i+N1,M+2} = \psi_{i,2} + \Delta\psi \text{ and } \psi_{i,1} = \psi_{i+N1,M+1} - \Delta\psi \tag{10}$$

Upstream of the cascade, $\Delta\psi$ in Eq. (10) is the difference in values between the two airfoils. Downstream of the cascade, $\Delta\psi$ is increased to account for wake displacement, which has the effect of a source. The amount of increase is determined from the trailing edge radius, the boundary-layer displacement, and the trailing edge velocity for each iteration:

$$\Delta\psi_{dn} = \Delta\psi_{up} + (2r_{te} + \delta_s^* + \delta_p^*) V_{te} \tag{11}$$

On the downstream boundary, the stream function is again assumed to be linear and is determined from the exit flow angle and the value at $i=NT$ and $j=M+2$. The exit flow angle is altered on each iteration to result in equal pressure on the suction and pressure sides of the airfoils.

Results

The preceding equations are solved simultaneously at each longitudinal position, beginning at the first station inside the upstream boundary and marching to the last. The elliptic effect of the inviscid flow equations is included by an iteration over the flowfield until the change between iterations is within an acceptable tolerance.

Results of the calculations for NACA 65-410 airfoils are compared with experimental data in Fig. 3. As can be seen, the results are highly encouraging, even with the relatively coarse rectangular grid (12×75) and the very approximate boundary-layer method. Details of the laminar boundary layer and transition have not been included in the present program, so a turbulent boundary layer was estimated near the leading edge. However, these simplifications are not necessary to the basic approach, the presentation of which is the objective of this Note.

Conclusions

A particular advantage of the present method is that stall can be approximated if a reasonable model for the separated turbulent boundary layer is included. This calculation for separated regions is stable with a simultaneous solution of the inviscid flow and an integral method for the boundary layers.

References

[1] Moses, H. L., Jones, R. R. III, O'Brien, W. F., Jr. and Peterson, R. S., "Simultaneous Solution of the Boundary Layer and Freestream with Separated Flow," *AIAA Journal*, Vol. 16, Jan. 1978, pp. 61-66.

[2] Moses, H. L., Sparks, J. F., and Jones, R. R. III, "An Integral Method for the Turbulent Boundary Layer with Separated Flow," *Turbulent Boundary Layers*, edited by H. E. Weber, ASME, New York, 1979, pp. 69-73.

[3] Jones, R. R., III, "The Performance Estimation of an Axial-Flow Compressor Stage Using Theoretically Derived Blade Element Characteristics with Experimental Comparison," Ph.D. Dissertation, Mechanical Engineering Dept., VPI&SU, Blacksburg, Va., 1979.

[4] Herrig, L. J., Emery, J. C., and Erwin, J. R., "Systematic Two-Dimensional Cascade Tests of NACA 65-Series Compressor Blades at Low Speeds," NACA TN-3916, 1957.

[5] Peterson, C. R., "Boundary Layer on an Airfoil in a Cascade," Gas Turbine Lab., MIT, Cambridge, Mass., Rept. 49, 1958.

AIAA 82-4239

Parallel Hydrogen Injection into Constant-Area, High-Enthalpy, Supersonic Airflow

R. J. Stalker* and R. G. Morgan†
University of Queensland, Brisbane, Australia

Introduction

In principle, the supersonic combustion ramjet offers a means of propulsion for future orbital launch vehicles, and for this purpose, it will be necessary to operate at flight speeds up to 6 km/s. Although mixing and burning of hydrogen injected into the combustion chamber are an essential part of the operation of such a scramjet, experimental investigations of this process have been limited to speeds of less than 2.2 km/s.[1] The experiments reported here were aimed at extending this limit, and were performed at stagnation enthalpies up to 13 MJ/kg, corresponding to a flight speed of approximately 5 km/s.

Experiments

The experiments were conducted in the Free-Piston Shock Tunnel T3[2] at the Australian National University. The tunnel was operated in the reflected shock mode and expanded the shock-heated test gas, from the stagnation region at the downstream end of the shock tube, through a conical nozzle with included divergence angle of 15 deg and an area ratio of 13, to a freejet test section.

The model combustion duct was designed to produce a flow that was essentially two-dimensional. A streamwise section of the duct is shown schematically in Fig. 1. It was of rectangular cross section, 25×50 mm, with the greater dimension horizontal. The intake had sharp leading edges and was located at a point in the test section flow where the Mach number was 3.5 and the static pressure approximately 120 kPa. The hydrogen injector strut had a sharp leading edge, with an included angle of 20 deg, and completely spanned the duct. The injection nozzle was two-dimensional, with a throat width of 1.6 mm, and produced a uniform spanwise mass flow distribution. From a point 18 mm downstream of the nozzle, the sidewalls were made of optical-quality glass.

Received Feb. 25, 1982.

*Professor, Dept. of Mechanical Engineering. Member AIAA.
†Research Fellow, Dept. of Mechanical Engineering

Hydrogen injection was controlled by a quick-opening valve, which produced a steady flow of hydrogen for 10 ms. By proper timing of the valve trigger, it was arranged that the steady flow of hydrogen was established prior to arrival of the test flow.

Mach-Zehnder interferograms were taken with a light source of 583 nm wavelength and 5 ns duration. Surface pressures also were obtained on the lower surface of the duct, using PCB quartz pressure transducers.

Results and Analysis

The time-resolved pressure records indicated that steady flow was established by 350 μs after shock reflection at the highest stagnation enthalpy tested and by 500 μs at the lowest. Pressure distributions were obtained approximately 100 μs after these times and are presented in Fig. 2.

As shown in Fig. 2a, flow disturbances from the injector gave rise to irregularities in the pressure distribution in the absence of injection, and these persisted when injection took place. Nevertheless, by obtaining the ratio

$$\Delta p = (p_i - p_0)/p_0$$

where p_i and p_0 are pressures with and without injection, respectively, an approximate measure of the pressure rise due to combustion was obtained. This is plotted in Figs. 2b-e. For Figs. 2b-d, estimated airstream temperatures were in excess of 2000 K, and ignition delay times were less than reaction times, which were less than 10 μs (Ref. 3) compared with airstream duct transit times of approximately 50 μs. Therefore, a significant degree of reaction occurred. For Fig. 2e, airstream temperature was 1000 K, ignition delay times were of the order of 100 μs (Ref. 3), and reaction did not take place. The distribution of Δp therefore was similar to that obtained when hydrogen is injected into a nitrogen stream.

Estimates of combustion-induced pressure rise were made, based upon a simplified diffusion flame theory.[4] Pressure gradients were neglected, only the reaction

$$2H_2 + O_2 \rightleftharpoons 2H_2O$$

was considered, and it was assumed that this took place at an infinitely thin flame front. Development of the two-dimensional turbulent jet downstream of the injector was first calculated on the assumption that the density remained

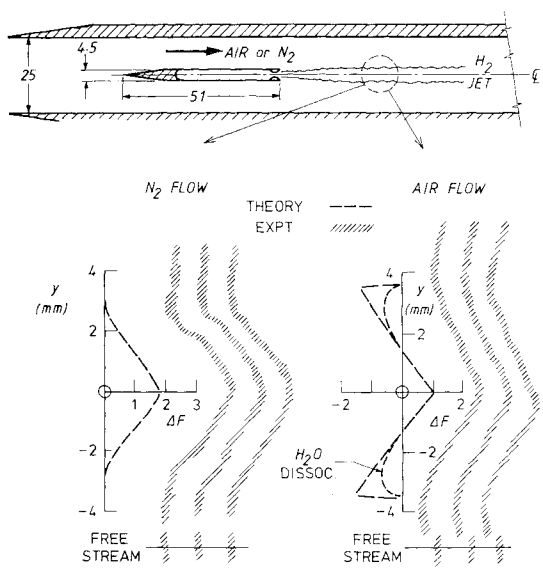

Fig. 1 Injector configuration and jet fringe shifts (stagnation enthalpy = 13 MJ/kg, equivalence ratio = 0.8, ΔF = fringe shift − freestream fringe shift, y = distance from centerline).